THE EUROPEAN
PHYSICAL JOURNAL C

Weak cosmic censorship in Born–Infeld electrodynamics and bound on charge-to-mass ratio

Tong-Tong Hu[a], Yan Song[b], Shuo Sun[c], Hong-Bo Li[d], Yong-Qiang Wang[e]

Research Center of Gravitation, Institute of Theoretical Physics, Key Laboratory for Magnetism and Magnetic of the Ministry of Education, Lanzhou University, Lanzhou 730000, China

Abstract We construct a class of counterexamples to cosmic censorship in four dimensional Einstein–Born–Infeld theory with asymptotically anti-de Sitter boundary conditions, and investigate the effect of the Born–Infeld parameter b in comparison with the counterpart of Einstein–Maxwell theory. When a charged massive scalar field is included into the action, we find that this class of counterexamples to cosmic censorship would be removed if the charge of scalar fields is above the bound of charge q_w. In particular, the bound of charge required to preserve cosmic censorship increases with the increasing of Born–Infeld parameter. Meanwhile, we also show the lower bounds on charge-to-mass ratio with the different values of Born–Infeld parameter.

Contents

1 Introduction

The study of black hole singularities has been an interesting subject since the original work on the weak cosmic censorship conjecture (WCCC) [1,2], which states naked singularities arising in the solutions of Einstein's equations [3] must be hidden within event horizons of black hole, and could not be observed from future null infinity. Although the concrete proof for the validity of WCCC has not been established, there exist lots of works of testing the validity of WCCC through the gedanken experiment [4], which was firstly proposed by Wald to destroy an extremal Kerr–Newman black hole by throwing a massive particle. Moreover, by considering the gravitational collapse of a scalar field, the authors in [5] firstly found that the final fate of a continual collapse would be a naked singularity. See [6] for a review. It's worth noting that time evolution of the matter field leads to formation of a naked singularity in finite time. Obviously, it is an interesting question to ask whether there exists a region of arbitrarily large curvature that is time-independent and observed to distant observers. It is well known that because in higher dimensions the event horizon of a class of black holes is not necessarily the case of topologically spherical surface, black holes would be unstable under gravitational perturbations in the region of the Gregory–Laflamme instability [7] and could produce a naked singularity, which implies the violation of cosmic censorship [8–10]. Besides, by analysing the non-linear evolution of black holes [11,12], one found that a naked singularity should form in finite time. In four dimensions, it is more difficult to construct the naked singularity. By investigating the model of Einstein gravity coupling to a Maxwell field with a negative cosmological constant [13,14], one obtained a class of counterexamples to cosmic censorship with asymptotically anti-de Sitter (AdS) boundary for the first time. Furthermore, considering the above model with a vanishing Maxwell field, the authors in Ref. [15] constructed smooth stationary solutions with differential rotation to the boundary metric, which also provides a possible vacuum counterexample to weak cosmic censorship in AdS spacetime.

[a] e-mail: hutt17@lzu.edu.cn

[b] e-mail: songy18@lzu.edu.cn

[c] e-mail: sunsh17@lzu.edu.cn

[d] e-mail: lihb2017@lzu.edu.cn

[e] e-mail: yqwang@lzu.edu.cn (corresponding author)

Springer

Recently, by introducing a charged scalar field to the Einstein–Maxwell solutions [16], the authors found that when the charge of the scalar field was sufficient large, the static solution of Einstein–Maxwell action would become unstable and a new stable solution could appear with nontrivial charged scalar field, which is analogous to the instability of a charged black hole to develop scalar condensation in the study of holographic superconductor [17–19]. Meanwhile, there exists a minimum value of charge required to remove the counterexamples and preserve cosmic censorship. It is surprising that the minimum value of charge appears to agree precisely with that proposed in the weak gravity conjecture [20], which states that any consistent quantum theory of gravity must have a stable state whose charge-to-mass ratio q/m is equal to or larger than that of an extremal black hole. In the case of Einstein–Maxwell model, the bound of q/m is equal to 1. To further test the weak gravity - cosmic censorship connection, the authors in [21] also studied the static solutions in Einstein theory with a dilaton field and the multi-charged scalar field case.

Considering that Maxwell theory is only the theory of linear electrodynamics, we would like to know whether or not there exists a class of counterexamples to cosmic censorship and the charge-to-mass ratio bound in four dimensional Einstein-nonlinear electrodynamics theory. The Born–Infeld electrodynamics [22–24] is a nonlinear generalization of the Maxwell's theory, which can remove the divergence of self-energy of a point-like charge in Maxwell electrodynamics. Moreover, the Lagrangian of Born–Infeld can arise from the low-energy effective theory describing electromagnetism [25,26]. Many works on the black holes solutions in Einstein–Born–Infeld theory have been studied in [27–34].

In the present paper, we show how to construct a class of counterexamples to cosmic censorship in four dimensional Einstein–Born–Infeld theory with asymptotically anti-de Sitter boundary. Furthermore, comparing with the counterpart of Einstein–Maxwell theory, we investigate the counterexample of Einstein–Born–Infeld theory for several values of Born–Infeld parameter b. Besides, introducing a charged massive scalar field into Einstein–Born–Infeld theory, we find that this class of counterexamples to cosmic censorship would be removed, and we also study the value of the lower bound on the scalar field charge required to preserve cosmic censorship in the case of Born–Infeld action.

The paper is organized as follows. In Sect. 2, we introduce the model of Einstein–Born–Infeld coupling to a complex, charged scalar field and the numerical DeTurck method. In Sect. 3, we explore the ansatz of metric and matter field, and analyze the boundary conditions. Numerical results of a class of counterexamples to cosmic censorship and static solutions with charged scalar condensation are shown in Sect. 4. The conclusion and discussion are given in the last section.

2 Set up

Let us begin with the action of the Born–Infeld field and a charged complex scalar field in the four-dimensional Einstein gravity spacetime with a negative cosmological constant, which is written as

$$S = \frac{1}{16\pi G} \int d^4x \sqrt{-g} \left[R + \frac{6}{L^2} + \mathcal{L}_{BI} \right. $$
$$\left. -4(\mathcal{D}_a\Phi)(\mathcal{D}^a\Phi)^\dagger - 4m^2\Phi\Phi^\dagger \right], \qquad (2.1)$$

where $\mathcal{L}_{BI} = \frac{4}{b}(1 - \sqrt{1 + \frac{bF}{2}})$ with the field strength of the U(1) gauge field $F = F_{ab}F^{ab}$, and L is the radius of asymptotic AdS spacetime. The constants m and q represent the mass and the charge of the complex scalar field , respectively. The constant b is the Born–Infeld parameter and the Born–Infeld field will reduce to the Maxwell case when $b \to 0$. Where $\mathcal{D}_a = \nabla_a - iqA_a$ is the gauge covariant derivative with respect to A_a. Note that the values of m^2 must satisfy the Breitenlohner–Freedman (BF) bound $m^2 \geq -9/4$ [35] for the (3+1)-dimensional spacetime.

The motion equations can derived from Eq. (2.1)

$$R_{ab} + \frac{3}{L^2}g_{ab} = T_{ab}, \qquad (2.2a)$$

$$\nabla_a(-\mathcal{F}F^a_b) = i q \left[(\mathcal{D}_b\Phi)\Phi^\dagger - (\mathcal{D}_b\Phi)^\dagger\Phi \right], \qquad (2.2b)$$

$$\mathcal{D}_a\mathcal{D}^a\Phi = m^2\Phi, \qquad (2.2c)$$

with the energy-momentum tensor of matter field

$$T_{ab} = 2\left(-\mathcal{F}F_a{}^cF_{bc} + \frac{g_{ab}}{4}\mathcal{L}_{BI} \right) + 2(\mathcal{D}_a\Phi)(\mathcal{D}_b\Phi)^\dagger$$
$$+ 2(\mathcal{D}_a\Phi)^\dagger(\mathcal{D}_b\Phi) + 2m^2g_{ab}\Phi\Phi^\dagger,$$

where $\mathcal{F} \equiv \frac{\partial\mathcal{L}_{BI}}{\partial F}$, and it equals to -1 in Maxwell condition.

If the complex, massive scalar field ψ vanishes, the solution of Einstein equations (2.2), which can describe the asymptotically spherically black hole with charge, is the well-known Born–Infeld AdS black hole. In terms of spherical coordinates, the metric of Born–Infeld AdS black hole is the following form

$$ds^2 = -f(r)dt^2 + f^{-1}(r)dr^2 + r^2(d\theta^2 + \sin^2\theta d\phi^2), \qquad (2.3)$$

with

$$f(r) = 1 - \frac{2M}{r} + \frac{r^2}{L^2} + \frac{4Q^2\,_2F_1(\frac{1}{4}, \frac{1}{2}; \frac{5}{4}; -\frac{bQ^2}{r^4})}{3r^2}$$
$$+ \frac{2r^2}{3b}\left(1 - \sqrt{\frac{bQ^2}{r^4} + 1} \right), \qquad (2.4)$$

where M and Q are the ADM mass and the electric charge of BI AdS black hole, respectively, and $_2F_1$ is a hypergeometric

function [37]. The gauge potential is

$$A = -\frac{Q_2 F_1(\frac{1}{4}, \frac{1}{2}; \frac{5}{4}; -\frac{bQ^2}{r^4})}{r} dt. \quad (2.5)$$

When there exists a non-trivial configuration of the complex scalar field, it is obvious that we should solve the equations of motion (2.2) numerically instead of seeking the analytical solutions. We will use DeTurk method to solve these equations, which provides a good tool for solving Einstein equations in these papers. By adding a gauge fixing term to Einstein equation (2.2a), we could obtain a set of elliptic equations, which are known as Einstein–DeTurk equation

$$R_{ab} + \frac{3}{L^2} g_{ab} - \nabla_{(a} \xi_{b)} = T_{ab}, \quad (2.6)$$

where $\xi^a = g^{bc}(\Gamma^a_{bc}[g] - \Gamma^a_{bc}[\tilde{g}])$ is the Levi–Civita connection associated with a reference metric $\tilde{g}$, which should be choose to be as same boundary and horizon structure as g.

3 Ansatz and boundary conditions

Motived by the coordinate systems used in [13,16,21,36], we also consider Poincaré coordinates for pure AdS spacetime,

$$ds^2 = \frac{L^2}{z^2}\left[-dt^2 + dr^2 + r^2 d\phi^2 + dz^2\right]. \quad (3.1)$$

When we use the new coordinate system,

$$z = \frac{y\sqrt{2 - y^2}}{1 - y^2}(1 - x^2), \quad (3.2a)$$

$$r = \frac{y\sqrt{2 - y^2}}{1 - y^2} x\sqrt{2 - x^2}, \quad (3.2b)$$

the metric (3.2) can become the following form:

$$ds^2 = \frac{L^2}{(1 - x^2)^2}\left[-\frac{(1 - y^2)^2 dt^2}{y^2(2 - y^2)} + \frac{4 dx^2}{2 - x^2}\right.$$
$$\left. + \frac{4 dy^2}{y^2(1 - y^2)^2(2 - y^2)^2} + x^2(2 - x^2) d\phi^2\right], \quad (3.3)$$

where x and y are polar-like coordinates. The Poincaré horizon is now located at y = 1, and the axis of rotation is located at x = 0. The conformal boundary is located at x = 1, and y = 0 denotes the intersection of the conformal boundary with the axis of symmetry.

In order to construct static, axisymmetric solutions with a timelike Killing vector and an axisymmetric Killing vector, we adopt the following ansatz of metric

$$ds^2 = \frac{L^2}{(1 - x^2)^2}\left[-\frac{(1 - y^2)^2 U_1 dt^2}{y^2(2 - y^2)}\right.$$
$$\frac{4 U_4}{2 - x^2}\left(dx + \frac{U_3}{1 - y^2} dy\right)^2$$
$$+ \frac{4 U_2 dy^2}{y^2(1 - y^2)^2(2 - y^2)^2}$$
$$\left. + x^2(2 - x^2) U_5 d\phi^2\right], \quad (3.4)$$

where the functions U_i ($i = 1, 2, 3, 4, 5$) depend on the variables x and y. Both of variables take values in [0, 1]. When $U_1 = U_2 = U_4 = U_5 = 1$ and $U_3 = 0$, the ansatz (3.4) can reduce to the pure AdS metric (3.3), which is the reference metric $\tilde{g}$ we take in DeTurk method.

Considering the above metric (3.4), an ansatz of matter fields should be described as below

$$A = LU_6 dt, \qquad \Phi = \left(1 - x^2\right)^\Delta y^\Delta \left(2 - y^2\right)^{\frac{\Delta}{2}} U_7 \quad (3.5)$$

with

$$\Delta \equiv 3/2 + \sqrt{9/4 + m^2}, \quad (3.6)$$

where the function U_6 and U_7 are the function of x and y. According to AdS/CFT duality, we take $\langle \mathcal{O}_2 \rangle = (1 - y^2)^2 U_7$ to describe the scalar condensation. To simplify, we only choose $m^2 = -2$ in our paper.

Next, we will discuss the boundary conditions. At conformal boundary, located at $x = 1$, the metric must reduce to pure AdS spacetime, so we must take

$$U_1(1, y) = U_2(1, y) = U_4(1, y) = U_5(1, y) = 1,$$
$$U_3(1, y) = 0, \quad (3.7)$$

and the boundary condition of scalar field is

$$\partial_x U_7(1, y) = 0, \quad (3.8)$$

which can be obtained by expanding the equations of motion near $x = 1$ as a power series in $(1 - x)$. For the gauge field at the boundary, we take

$$U_6(1, y) = a(1 - y^2)^n, \quad n = 2, 4, 6, \ldots, \quad (3.9)$$

where the constant a is the amplitude. This kind of profile for gauge field has been studied in [13,16,21,36].

The asymptotic behaviors of the equations of motion near $x = 0$ give the conditions at $x = 0$:

$$\frac{\partial U_1}{\partial x} = \frac{\partial U_2}{\partial x} = \frac{\partial U_4}{\partial x} = \frac{\partial U_5}{\partial x}$$
$$= \frac{\partial U_6}{\partial x} = \frac{\partial U_7}{\partial x} = 0,$$
$$U_3(0, y) = 0, \quad U_4(0, y) = U_5(0, y). \quad (3.10)$$

At $y = 0$, i.e. the intersection of the conformal boundary with the axis of symmetry, we set the boundary conditons

$$U_1(x, 0) = U_2(x, 0) = U_4(x, 0) = U_5(x, 0) = 1,$$
$$U_3(x, 0) = \partial_y U_7(x, 0) = 0,$$
$$U_6(x, 0) = a, \qquad (3.11)$$

and at Poincaré horizon y=1, Dirichlet boundary conditions are imposed on

$$U_1(x, 1) = U_2(x, 1) = U_4(x, 1) = U_5(x, 1) = 1,$$
$$U_3(x, 1) = U_6(x, 1) = U_7(x, 1) = 0. \qquad (3.12)$$

4 Numerical results

In this section, we will numerically solve the coupled system of nonlinear partial differential equations (2.2) with the ansatzs (3.4) and (3.5). We employ finite element methods in the integration region $0 \leq x \leq 1$ and $0 \leq y \leq 1$ defined on non-uniform grids, allowing the grids to be more finer grid points near the boundary of $y = 0$ and $y = 1$. Our iterative process is the Newton–Raphson method. The relative error for the numerical solutions in this work is estimated to be below 10^{-5}. In order to keep good agreement with the aforementioned error, the grid size has to be increased and typically a 120×200 to 120×300 grid was used.

We would study the following two cases with scalar field $\Phi = 0$ and $\Phi \neq 0$, respectively. For convenience, in the following results, we will set $L = 1$.

4.1 With charged scalar field $\Phi = 0$

In this subsection, we will analyze the solutions with charged scalar field $\Phi = 0$ and present the evidence for counterexample to cosmic censorship. When one obtains a solution of Einstein equations, it is important to investigate whether or not the spacetime of solution is regular. In general, one of the most useful ways is to check for the finiteness of the Kretschmann scalar, which is also called Riemann tensor squared and written as

$$K = R_{\alpha\beta\gamma\delta} R^{\alpha\beta\gamma\delta}, \qquad (4.1)$$

where $R_{\alpha\beta\gamma\delta}$ is the Riemann curvature tensor. Therefore, Kretschmann scalar is a sum of squares of tensor components and a quadratic invariant.

Numerical results are presented in Fig. 1. In the left panel we present the distribution of Kretschmann scalar K as a function of x and y coordinate with $b = 0.25$, $n = 8$ and $a = 6$. It is obvious that the spacetime is not flat, and the value of the Kretschmann scalar in the purple area is about to $24/L^4$, which means it recovers the result of AdS_4 spacetime. In addition, the maximum of the Kretschmann scalar appears

Table 1 Maximum amplitude a_{max} for several values of n and b

b	a_{max}			
	n			
	4	6	8	10
0.00	4.95	6.53	8.06	9.13
0.25	4.22	5.51	6.56	7.45
0.5	3.82	4.99	5.94	6.76
1	3.35	4.36	5.20	5.91

at the boundary $x = 0$. In the right panel, we exhibit the maximum of the Kretschmann scalar K versus the amplitude a with the fixed Born–Infeld parameters $b = 0$, 0.25, 0.5, represented by the black, blue and green lines, respectively. The vertical black, blue and cyan dashed gridlines indicate $a_{max} = 8.06$, 6.56 and 5.94, respectively, and the horizontal red line is the value of $K = 24$ for AdS_4 spacetime. From the figure, we could find that when the Born–Infeld parameters $b \neq 0$, there still exists the growth of the maximum of Kretschmann scalar with the increasing of a, which indicates the formation of a curvature singularity similar to the case of Maxwell action in [16].

When the amplitude reaches to a maximum value, there will appear a singularity, which means producing arbitrarily large curvature in spacetime. This maximum depends on both n and b. We show our results in the following table.

From Table 1, we could see that the maximum amplitude a_{max} increases with the increasing of n. Meanwhile, it decreases with the increasing of the Born–Infeld parameter b. When Maxwell field is extended to Born–Infeld model, the static solutions could still become singular at a finite value of a.

4.2 With charged scalar field $\Phi \neq 0$

In the last subsection, we obtain a family of Einstein–Born–Infeld solutions with charged scalar field $\Phi = 0$. We would like to know whether or not there exist the charged static solutions with no-vanished scalar field, which is analogous to the case of holographic superconductor studied in [17,19,38,39]. When fixed the parametes b and a, there is a minimal value of q, below which the scalar field vanishes and the solution is the simple planar. Above this value, the charged static solution becomes unstable to develop scalar hair. To obtain the minimal value of the charge q, we could use the method in [16,40] to treat the equation of motion of Φ perturbatively. Therefore, before numerically solving the full dynamic equations of motion including scalar field in Eqs. (2.2), we solve the time-independent scalar field equations to search for zero mode at the fixed background constructed in Sect. 4.1,

$$(\nabla_a \nabla^a - m^2)\Phi = q^2 A_a A^a \Phi, \qquad (4.2)$$
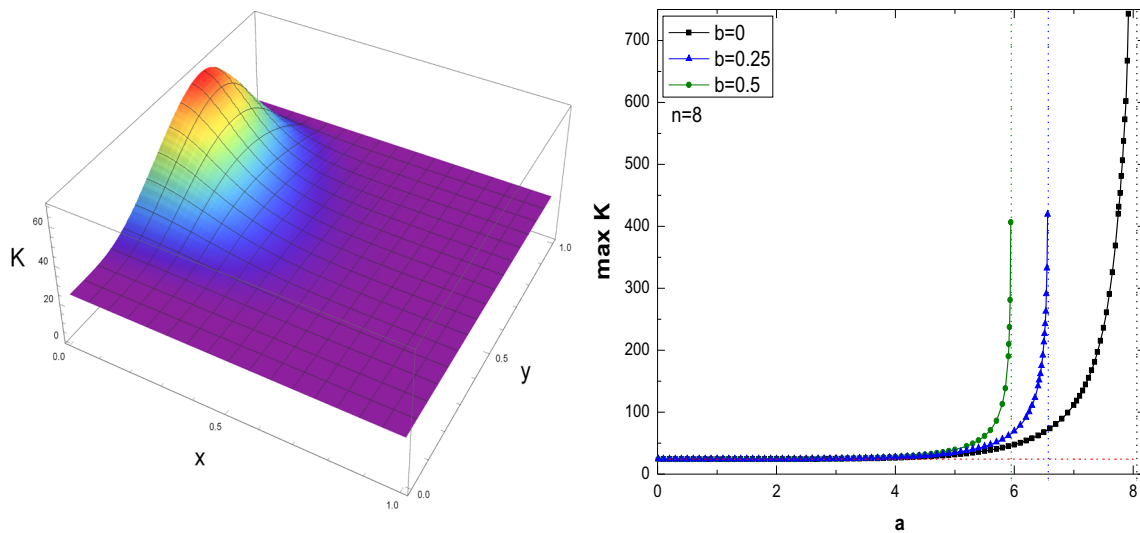
Fig. 1 Left: The distribution of Kretschmann scalar as a function of x and y coordinate with $b = 0.25$, $n = 8$ and $a = 6$. Right: The maximum of the Kretschmann scalar as a function of a with the fixed Born–Infeld parameters $b = 0$, 0.25, 0.5, represented by the black, blue and cyan lines, respectively. The vertical black, blue and cyan dashed gridlines indicate $a_{max} = 8.06$, $a_{max} = 6.56$ and $a_{max} = 5.94$, respectively, and the horizonal red line is the value of $K = 24$ for AdS$_4$ spacetime

which one could recognize as an eigenvalue problem with the eigenfunction Φ and eigenvalue q^2. We will use q_{min} to denote the smallest eigenvalue of zero-mode, which is the minimal charge and is also a function of the amplitude a.

The results are shown in Fig. 2. In left panel, with the fixed $n = 8$, we plot minimal charge q_{min} as a function of the amplitude a for the corresponding values of $b = 1, 0.5, 0.25$ and 0, represented by cyan, blue, red and black lines, respectively. The vertical dashed gridlines indicate the maximum amplitude $a_{max} = 8.06$ (black), 6.56 (red), 5.94 (blue) and 5.20 (cyan), respectively, which corresponds to the values of $n = 8$ shown in Table 1. For each curve, the minimal charge q_{min} decreases with the increasing of amplitude a. We see that for the fixed amplitude a, the critical charge q_{min} increases with the increasing of Born–Infeld parameter b. Furthermore, when the amplitude a decreases, the minimal charge q_{min} tends to the same value for several values of b.

In the right of Fig. 2, with the fixed $b = 0.25$, we plot minimal charge q_{min} as a function of the amplitude a for the corresponding values of $n = 10, 8, 6$ and 4, represented by cyan, blue, red and black lines, respectively. For each curve, the minimal charge q_{min} decreases with the increasing of amplitude a, which is similar to the behavior in the left panel. For the fixed amplitude a, the minimal charge q_{min} increases with the increasing of n.

Next, we could solve the coupled equations of motion (2.2) to find the solutions for the above critical charge q_{min}. We show the profiles of the expectation value for the operator dual to Φ as a function of the boundary radial coordinate r in Fig. 3. In the left panel, with the fixed $n = 8$ and $q = 2.7$,

the curves from top to bottom correspond to $b = 0, 0.5, 1$, represented by black, red and blue lines, respectively. For each curve, the scalar condensation $\langle \mathcal{O}_2 \rangle$ decreases with the increasing amplitude of r. When the amplitude r increases, the scalar condensation tends to zero value for several values of b. Moreover, at the origin $r = 0$, there exists the largest value of the scalar condensation. Furthermore, for the fixed amplitude r, the scalar condensation $\langle \mathcal{O}_2 \rangle$ decreases with the increasing value of Born–Infeld parameter b.

In the right of Fig. 3, with the fixed $b = 0.25$ and $q = 2.22$, we plot the scalar condensation $\langle \mathcal{O}_2 \rangle$ as a function of r for several values of a. The curves from top to bottom correspond to $a = 10, 9, 8, 7$ and 5.8, represented by black, red, blue, cyan and purple lines, respectively. For each curve, the scalar condensation decreases with the increasing of r, which is similar to the behavior in the left panel. For the fixed amplitude b, the scalar condensation $\langle \mathcal{O}_2 \rangle$ increases with the increasing value of the parameter a.

In order to further understand how increasing the amplitude a affects the maximum of the condensation with the different values of b, we show in the left panel of Fig. 4 the condensate $\langle \mathcal{O}_2 \rangle$ at $r = 0$ as a function of the amplitude a with the fixed parameters $n = 8$, $q = 2.7$. From top to bottom, the curves correspond to the values of $b = 0$, $b = 0.5$, and $b = 1$, respectively. In addition, the vertical dashed gridlines indicate the critical amplitude $a_c = 4.74$ (black), $a_c = 4.82$ (red) and $a_c = 4.98$ (blue), respectively. As one can see that there exists a critical amplitude a_c above which the condensate appears, then rises as the system is imposed with much larger amplitudes a. This behaviour of
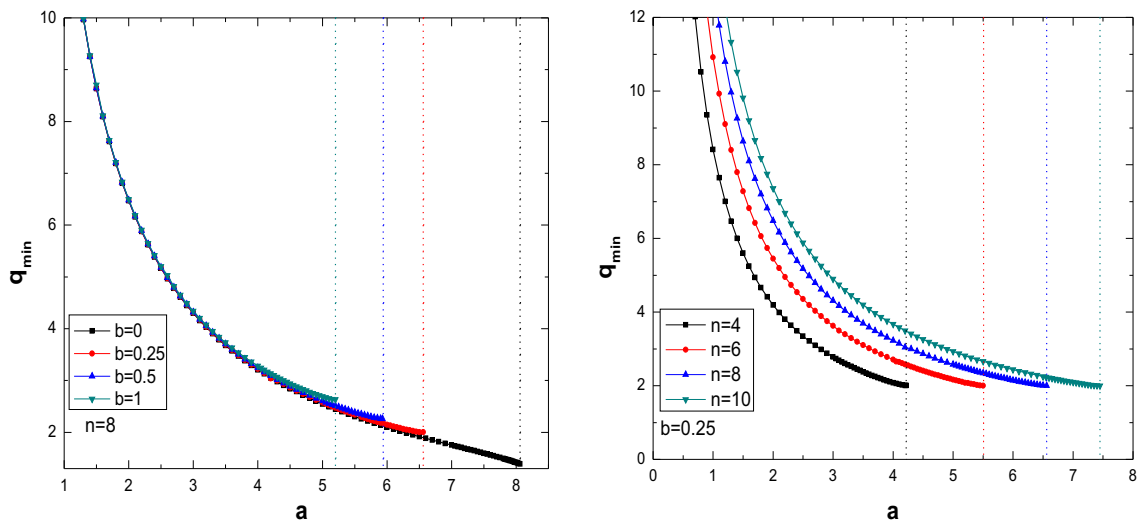
Fig. 2 The minimal charge q_{min} as a function of the amplitude a. Left: For the fixed $n = 8$, the curves from top to bottom correspond to $b = 1, 0.5, 0.25, 0$, respectively. Right: For the fixed $b = 0.25$, the curves from top to bottom correspond to $n = 10, 8, 6, 4$, respectively
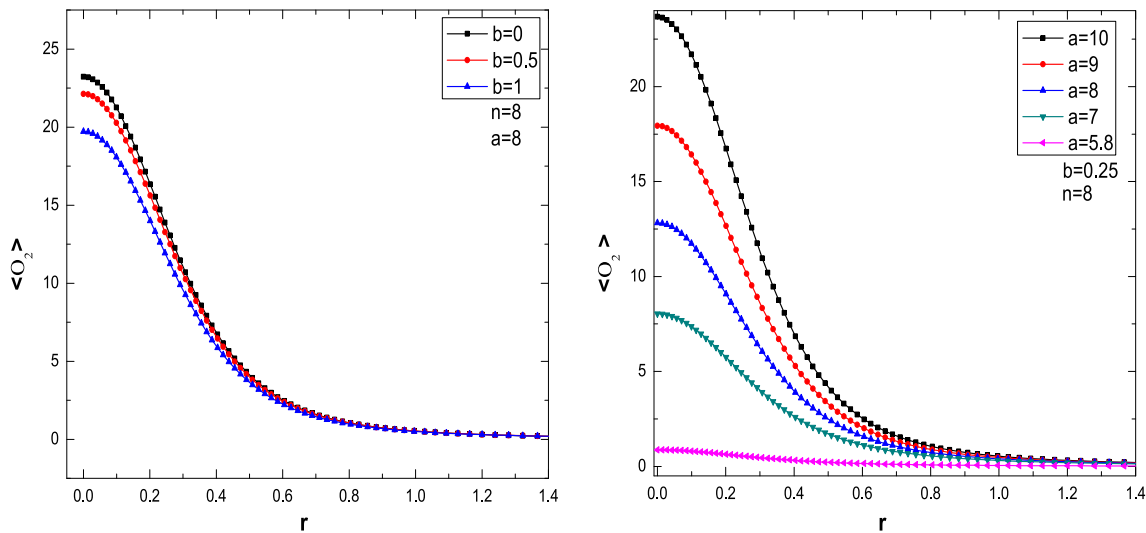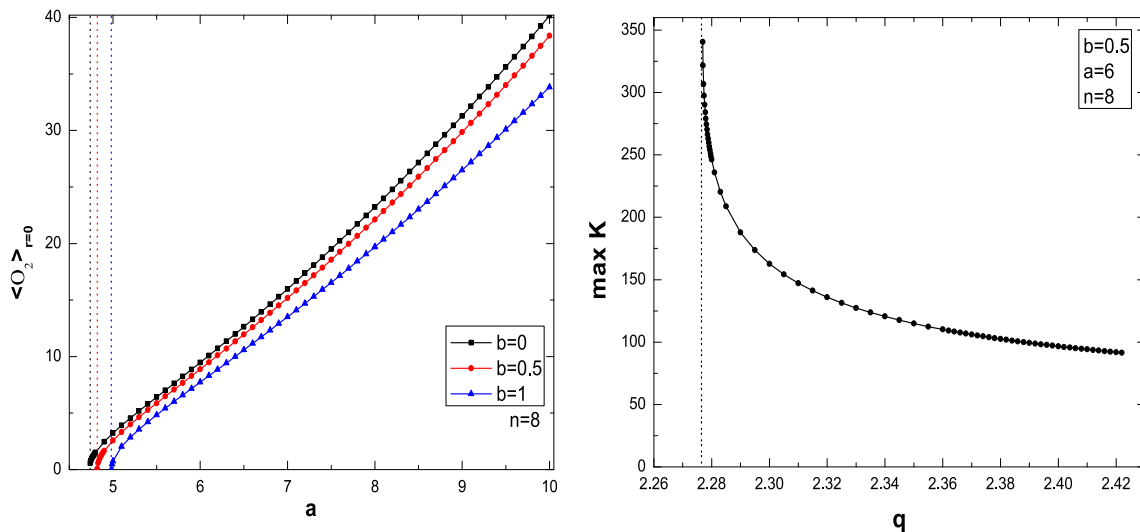

Fig. 3 The condensation as a function of radial coordinate r at conformal boundary with different b (left) and n (right). At both of these two figures we take the value of $n = 8$

$b \neq 0$ is qualitatively similar to that in Maxwell theory with $b = 0$.

After obtaining the numerical solution with charged scalar condensate, we want to know what happens to the solutions with $\Phi \neq 0$ as the decreasing of charge q when $a > a_{max}$. We present in the right panel of Fig. 4 the typical maximal value of Kretschmann scalar K as a function of the charge q with $b = 0.5$, $n = 8$ and $a = 6 > a_{max}$, and the vertical black dashed gridlines indicate the $q_{min} = 2.276$. From this plot, we can see that the full nonlinear solutions with the scalar condensate are in the range of $q > q_{min}$. It is obvious that there exists the growth of the maximum of Kretschmann scalar with the decreasing of q, which indicates the formation of a curvature singularity outside Poincaré horizon at

some minimal values $q = q_{min}$, and is similar to the case of Maxwell case.

To study the properties of the bound on charge-to-mass ratio, we exhibit the phase diagram of the minimal charge q_{min} versus the amplitude a with several values of Born–Infeld parameter in Fig. 5, where we add the curves of minimal charge with $a > a_{max}$ to previous plot for $a < a_{max}$ in the left panel of Fig. 2. The Born–Infeld parameters $b = 0.25, 0.5, 1$ are represented by the red, blue and orange lines, respectively. The black line represents the curve in the Maxwell model which has been discussed in [16]. We can see that there exists an asymptotical value q_w of q_{min} as a increases. The asymptotical value q_w increases with the increasing of Born–Infeld parameter b. More details

Fig. 4 Left: The condensation against a with different values of b at r = 0. Right: The typical maximal value of Kretschmann scalar K as a function of the charge q with $b = 0.5$, $n = 8$ and $a = 6$

are shown in the inset, and the horizonal black, red, blue and orange dashed gridlines indicate the values of $q_w = 2, 2.23, 2.43, 2.708$, respectively. If we consider scalar field with $q < q_w$, there still exists a singularity outside the Poincaré horizon as a increases to a finite value. But for keeping $q > q_w$, there would not exist a singularity when one increases the amplitude a to an arbitrarily large value.

It is noteworthy that for the curve of Maxwell model in the solutions with $\Phi \neq 0$, the minimal charge q_{min} decreases firstly with the decreasing of the amplitude a, and then it reaches a minimal point. Further increasing a to a_{max}, the value of q_{min} continues to decrease, and a second branch with lower q_{min} is obtained. When the curve with lower q_{min} moves toward a_{max}, the numerical error begins to increase and a finer mesh is required to calculate. It is difficult to handle numerical calculation near the value of a_{max}, so we could not get the curve connecting the solutions of $\Phi = 0$ and $\Phi \neq 0$. However, for larger value of b, it is relatively easy to obtain the connected curve near the value of a_{max}.

5 Conclusions

In this paper, we have presented a class of counterexamples to cosmic censorship in four-dimensional Einstein–Born–Infeld theory. The maximum of Kretschmann scalar goes to infinite when the amplitude a increases to a_{max}, which means there appears a singularity outside Poincaré horizon. If we consider the charged scalar field in this model, we found there exists a minimal value of charge q_{min}, below which the static solution with zero scalar condensation is stable. However, when the charge of the scalar field was above q_{min}, the static solution of Born–Infeld action will become unsta-
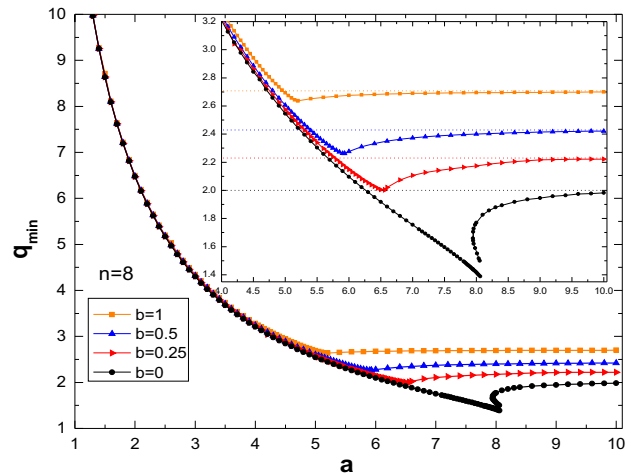
Fig. 5 The full phase diagram of q_{min} against a with the Born–Infeld parameters $b = 0.25, 0.5, 1$, represented by the red, blue and orange lines, respectively. The black line corresponds to the case of the Maxwell model

ble and a new stable solution with nontrivial charged scalar field could appear, which is analogous to the instability of a charged static solution to develop scalar condensation in the case of Maxwell theory [16]. Meanwhile, there exists the asymptotical value of charge q_w required to remove the counterexamples and preserve cosmic censorship. Comparing with the Einstein–Maxwell model, the bound of charge-to-mass ratio q/m is larger than 1 and increases with the Born–Infeld parameter b.

In the case of Maxwell theory [16], it is surprising to find that the bound of the charge to mass ratio which is necessary to preserve weak cosmic censorship is precisely equal to the weak gravity bound. For the nonlinear Born–Infeld theory,

we also obtain the the bound of the charge to mass ratio necessary to preserve weak cosmic censorship, but, because now the weak gravity conjecture in Born–Infeld electrodynamics is still not clear, one could not determine whether bound of charge-to-mass ratio is equal to weak gravity conjecture. However, it is sure that a class of static solution with charged scalar condensate could prevent the violation of the weak cosmic censorship, and the bound of charge-to-mass ratio could also be obtained in the case of Born–Infeld electrodynamic.

It will be interesting to investigate the several further researches. First, since we have studied the static solution with a free scalar condensate in Born–Infeld electrodynamic, we would like to investigate how self-interactions of the scalar field to prevent the violation of the weak cosmic censorship and the bound of charge-to-mass ratio. The second extension of our study is to construct generalized multi-scalar hair configurations, such as two coexisting states of the charge scalar field presented in Born–Infeld electrodynamic. Finally, we are planning to study the model of the Einstein–Born–Infeld-vector model and construct the static solution with charged vector hair necessary to preserve weak cosmic censorship in future work.

Data Availability Statement This manuscript has no associated data or the data will not be deposited. [Authors' comment: The datasets generated during the current study are available from the corresponding author on reasonable request.]

References

1. R. Penrose, Gravitational collapse: the role of general relativity. Riv. Nuovo Cim. **1**, 252 (1969)

2. R. Penrose, Gen. Rel. Grav. **34**, 1141 (2002)

3. S.W. Hawking, Breakdown of predictability in gravitational collapse. Phys. Rev. D **14**, 2460 (1976). https://doi.org/10.1103/PhysRevD.14.2460

4. R.M. Wald, Gedanken experiments to destroy a black hole. Ann. Phys. **82**, 548 (1974)

5. M.W. Choptuik, Universality and scaling in gravitational collapse of a massless scalar field. Phys. Rev. Lett. **70**, 9 (1993). https://doi.org/10.1103/PhysRevLett.70.9

6. P.S. Joshi, D. Malafarina, Recent developments in gravitational collapse and spacetime singularities. Int. J. Mod. Phys. D **20**, 2641 (2011). https://doi.org/10.1142/S0218271811020792. arXiv:1201.3660 [gr-qc]

7. R. Gregory, R. Laflamme, Black strings and p-branes are unstable. Phys. Rev. Lett. **70**, 2837 (1993). https://doi.org/10.1103/PhysRevLett.70.2837. arXiv:hep-th/9301052

8. V.E. Hubeny, M. Rangamani, Unstable horizons. JHEP **0205**, 027 (2002). https://doi.org/10.1088/1126-6708/2002/05/027. arXiv:hep-th/0202189

9. L. Lehner, F. Pretorius, Black strings, low viscosity fluids, and violation of cosmic censorship. Phys. Rev. Lett. **105**, 101102 (2010). https://doi.org/10.1103/PhysRevLett.105.101102. arXiv:1006.5960 [hep-th]

10. J.E. Santos, B. Way, Neutral black rings in five dimensions are unstable. Phys. Rev. Lett. **114**, 221101 (2015). https://doi.org/10.1103/PhysRevLett.114.221101. arXiv:1503.00721 [hep-th]

11. P. Figueras, M. Kunesch, S. Tunyasuvunakool, End point of black ring instabilities and the weak cosmic censorship conjecture. Phys. Rev. Lett. **116**(7), 071102 (2016). https://doi.org/10.1103/PhysRevLett.116.071102. arXiv:1512.04532 [hep-th]

12. P. Figueras, M. Kunesch, L. Lehner, S. Tunyasuvunakool, End point of the ultraspinning instability and violation of cosmic censorship. Phys. Rev. Lett. **118**(15), 151103 (2017). https://doi.org/10.1103/PhysRevLett.118.151103. arXiv:1702.01755 [hep-th]

13. G.T. Horowitz, J.E. Santos, B. Way, Evidence for an electrifying violation of cosmic censorship. Class. Quant. Grav. **33**(19), 195007 (2016). https://doi.org/10.1088/0264-9381/33/19/195007. arXiv:1604.06465 [hep-th]

14. T. Crisford, J.E. Santos, Violating the weak cosmic censorship conjecture in four-dimensional anti-de sitter space. Phys. Rev. Lett. **118**(18), 181101 (2017). https://doi.org/10.1103/PhysRevLett.118.181101. arXiv:1702.05490 [hep-th]

15. T. Crisford, G.T. Horowitz, J.E. Santos, Attempts at vacuum counterexamples to cosmic censorship in AdS. JHEP **1902**, 092 (2019). https://doi.org/10.1007/JHEP02(2019)092. arXiv:1805.06469 [hep-th]

16. T. Crisford, G.T. Horowitz, J.E. Santos, Testing the weak gravity - cosmic censorship connection. Phys. Rev. D **97**(6), 066005 (2018). https://doi.org/10.1103/PhysRevD.97.066005. arXiv:1709.07880 [hep-th]

17. S.S. Gubser, Breaking an Abelian gauge symmetry near a black hole horizon. Phys. Rev. D **78**, 065034 (2008). https://doi.org/10.1103/PhysRevD.78.065034. arXiv:0801.2977 [hep-th]

18. S.A. Hartnoll, C.P. Herzog, G.T. Horowitz, Building a holographic superconductor. Phys. Rev. Lett. **101**, 031601 (2008). https://doi.org/10.1103/PhysRevLett.101.031601. arXiv:0803.3295 [hep-th]

19. R.G. Cai, L. Li, L.F. Li, R.Q. Yang, Introduction to holographic superconductor models. Sci. China Phys. Mech. Astron. **58**(6), 060401 (2015). https://doi.org/10.1007/s11433-015-5676-5. arXiv:1502.00437 [hep-th]

20. N. Arkani-Hamed, L. Motl, A. Nicolis, C. Vafa, The string landscape, black holes and gravity as the weakest force. JHEP **0706**, 060 (2007). https://doi.org/10.1088/1126-6708/2007/06/060. arXiv:hep-th/0601001

21. G. T. Horowitz, J. E. Santos, Further evidence for the weak gravity - cosmic censorship connection, arXiv:1901.11096 [hep-th]

22. M. Born, Modified field equations with a finite radius of the electron. Nature **132**, 282–282 (1933)

23. M. Born, Quantum theory of the electromagnetic field. Proc. R. Soc. A **143**, 410–37 (1934)

24. M. Born, L. Infeld, Foundations of the new field theory. Proc. R. Soc. Lond. A **144**, 425 (1934). https://doi.org/10.1098/rspa.1934.0059

25. E.S. Fradkin, A.A. Tseytlin, Nonlinear electrodynamics from quantized strings. Phys. Lett. **163B**, 123 (1985). https://doi.org/10.1016/0370-2693(85)90205-9

26. R.G. Leigh, Dirac–Born–Infeld action from dirichlet sigma model. Mod. Phys. Lett. A **4**, 2767 (1989). https://doi.org/10.1142/S0217732389003099

27. A. García, H. Salazar, J.F. Plebánski, Type-D solutions of the Einstein and Born–Infeld nonlinear-electrodynamics equations. Nuovo Cimento B **84**, 65 (1984)

28. M. Cataldo, A. Garcia, Three dimensional black hole coupled to the Born–Infeld electrodynamics. Phys. Lett. B **456**, 28 (1999). https://doi.org/10.1016/S0370-2693(99)00441-4. arXiv:hep-th/9903257

29. S. Fernando, D. Krug, Charged black hole solutions in Einstein–Born–Infeld gravity with a cosmological constant. Gen. Rel. Grav. **35**, 129 (2003). https://doi.org/10.1023/A:1021315214180. arXiv:hep-th/0306120

30. T.K. Dey, Born–Infeld black holes in the presence of a cosmological constant. Phys. Lett. B **595**, 484 (2004). https://doi.org/10.1016/j.physletb.2004.06.047. arXiv:hep-th/0406169

31. R.G. Cai, D.W. Pang, A. Wang, Born–Infeld black holes in (A)dS spaces. Phys. Rev. D **70**, 124034 (2004). https://doi.org/10.1103/PhysRevD.70.124034. arXiv:hep-th/0410158

32. S. Li, H. Lu, H. Wei, Dyonic (A)dS black holes in Einstein–Born–Infeld theory in diverse dimensions. JHEP **1607**, 004 (2016). https://doi.org/10.1007/JHEP07(2016)004. arXiv:1606.02733 [hep-th]

33. P. Wang, H. Wu, H. Yang, Thermodynamics and phase transition of a nonlinear electrodynamics black hole in a cavity, arXiv:1901.06216 [gr-qc]

34. P. Wang, H. Wu, H. Yang, Thermodynamics and weak cosmic censorship conjecture in nonlinear electrodynamics black holes via charged particle absorption, arXiv:1904.12365 [gr-qc]

35. P. Breitenlohner, D.Z. Freedman, Stability in gauged extended supergravity. Ann. Phys. **144**, 249 (1982)

36. G.T. Horowitz, N. Iqbal, J.E. Santos, B. Way, Hovering black holes from charged defects. Class. Quant. Grav. **32**, 105001 (2015). https://doi.org/10.1088/0264-9381/32/10/105001. arXiv:1412.1830 [hep-th]

37. M. Abramowitz, I.A. Stegun, *Handbook of Mathematical Functions* (Dover, New York, 1972)

38. P. Basu, A. Mukherjee, H.H. Shieh, Supercurrent: vector Hair for an AdS black hole. Phys. Rev. D **79**, 045010 (2009). https://doi.org/10.1103/PhysRevD.79.045010. arXiv:0809.4494 [hep-th]

39. S.A. Hartnoll, C.P. Herzog, G.T. Horowitz, Holographic superconductors. JHEP **0812**, 015 (2008). https://doi.org/10.1088/1126-6708/2008/12/015. arXiv:0810.1563 [hep-th]

40. G.T. Horowitz, J.E. Santos, General relativity and the cuprates. JHEP **1306**, 087 (2013). https://doi.org/10.1007/JHEP06(2013)087. arXiv:1302.6586 [hep-th]